


Role of Imaging in Cardiomyopathies

Vincenzo Castiglione,^{1,2} Alberto Aimò,^{1,2} Giancarlo Todiere,¹ Andrea Barison,^{1,2} Iacopo Fabiani,¹ Giorgia Panichella,¹ Dario Genovesi,¹ Lucrezia Bonino,¹ Alberto Clemente,¹ Filippo Cademartiri,¹ Alberto Giannoni,^{1,2} Claudio Passino,^{1,2} Michele Emdin^{1,2} and Giuseppe Vergaro ^{1,2}

1. Cardiothoracic Department, Fondazione Toscana Gabriele Monasterio, Pisa, Italy; 2. Health Science Interdisciplinary Center, Scuola Superiore Sant'Anna, Pisa, Italy

Abstract

Imaging has a central role in the diagnosis, classification, and clinical management of cardiomyopathies. While echocardiography is the first-line technique, given its wide availability and safety, advanced imaging, including cardiovascular magnetic resonance (CMR), nuclear medicine and CT, is increasingly needed to refine the diagnosis or guide therapeutic decision-making. In selected cases, such as in transthyretin-related cardiac amyloidosis or in arrhythmogenic cardiomyopathy, the demonstration of histological features of the disease can be avoided when typical findings are observed at bone-tracer scintigraphy or CMR, respectively. Findings from imaging techniques should always be integrated with data from the clinical, electrocardiographic, biomarker, genetic and functional evaluation to pursue an individualised approach to patients with cardiomyopathy.

Keywords

Imaging, cardiomyopathies, echocardiography, cardiac magnetic resonance, nuclear medicine

Disclosure: The authors have no conflicts of interest to declare.

Received: 31 August 2022 **Accepted:** 7 November 2022 **Citation:** *Cardiac Failure Review* 2023;9:e08. **DOI:** <https://doi.org/10.15420/cfr.2022.26>

Correspondence: Giuseppe Vergaro, Scuola Superiore Sant'Anna and Fondazione Toscana Gabriele Monasterio, Via Moruzzi, 1 56124 Pisa, Italy.
E: giuseppe1.vergaro@santannapisa.it

Open Access: This work is open access under the CC-BY-NC 4.0 License which allows users to copy, redistribute and make derivative works for non-commercial purposes, provided the original work is cited correctly.

Imaging and Cardiomyopathy Phenotype

Cardiomyopathies (CMPs) are a group of diseases affecting the cardiac muscle, heterogeneous in terms of aetiology and clinical presentation. In 2008, a European Society of Cardiology (ESC) position statement defined CMPs as myocardial disorders “in which the heart muscle is structurally and functionally abnormal, in the absence of coronary artery disease, hypertension, valvular disease and congenital heart disease sufficient to cause the observed myocardial abnormality”.¹

CMPs were grouped into specific morphological and functional phenotypes (hypertrophic, dilated, arrhythmogenic, restrictive, or other CMPs), and each phenotype was sub-classified into familial/genetic and non-familial/non-genetic forms.¹ CMPs present variable expressions and symptoms, which may change over time.

CMPs may represent a challenge for cardiologists and imaging specialists, but an in-depth knowledge of aetiologies and characteristic features can lead to the correct diagnosis. The diagnostic workup of patients with suspected CMP includes clinical history and physical examination, a 12-lead ECG, specific laboratory tests, and often an endomyocardial biopsy and genetic testing. Cardiac imaging plays a pivotal role in the diagnosis of CMPs and their differentiation from mimicking conditions, such as athlete's heart. Transthoracic echocardiography (TTE) is a safe, readily available technique that may raise the suspicion of CMP or allow a first assessment of patients with suspected CMP. Other imaging modalities, such as cardiac magnetic resonance (CMR), cardiac CT (CCT) and nuclear

imaging, may help come to the correct diagnosis. In some cases, imaging findings alone are sufficient to diagnose specific disorders with no need for histological demonstration. The most notable case is amyloid transthyretin (ATTR) cardiac amyloidosis (CA), which can be diagnosed when there is an intense myocardial uptake of bone tracers on scintigraphy, and no monoclonal protein is found.²

Besides aetiological diagnosis, imaging techniques may help detect cardiac involvement in an earlier stage, characterise the remodelling pattern, perform an accurate functional assessment and risk stratification, and finally guide therapeutic decisions. TTE also offers the possibility of serial examinations over time. When possible, basic TTE examination should be integrated by speckle-tracking imaging of the left ventricle (LV), and, ideally, also of other cardiac chambers. CMR provides additional anatomical and functional information and enables tissue characterisation, which has important prognostic implications. Other techniques, such as CCT, scintigraphy or PET, may provide additional information to predict future disease trajectories and guide patient management.³ *Table 1* provides an overview of the utility of different imaging modalities for the assessment of CMPs.

Overall, multimodality cardiac imaging plays an important role in clinical decision-making and helps to improve patients' management and outcomes. In this review, we provide an overview of the current applications and some future perspectives on the use of imaging techniques in the diagnosis and treatment of patients with CMPs.

Table 1: Utility of Different Imaging Modalities for the Assessment of Cardiomyopathies

	TTE	CMR	SPECT	PET	CCT
Morphologic assessment	++	+++	+	+	++
Systolic and diastolic function	+++	+++	+	+	+
Valve disease	+++	++	-	-	+
Tissue characterisation	+	+++	-	-	+
Main applications	<ul style="list-style-type: none"> Main imaging technique for the initial assessment of patients with suspected CMP Risk stratification Main imaging technique during follow-up 	<ul style="list-style-type: none"> Gold standard for chamber quantification Differential diagnosis Risk stratification 	<ul style="list-style-type: none"> Non-biopsy diagnosis of ATTR-CA with ^{99m}Tc-labelled bone tracers 	<ul style="list-style-type: none"> Detecting inflammatory process (¹⁸F-FDG PET for sarcoidosis diagnosis and treatment monitoring) 	<ul style="list-style-type: none"> Rule out coronary artery disease
Main limitations	<ul style="list-style-type: none"> Acoustic window limitation Operator dependency 	<ul style="list-style-type: none"> Availability Metallic implants Use of contrast Low quality in arrhythmias or poor breath-holding ability 	<ul style="list-style-type: none"> Radiation exposure Attenuation artefacts 	<ul style="list-style-type: none"> Radiation exposure Availability Cost 	<ul style="list-style-type: none"> Radiation exposure Low quality in arrhythmias

Number of crosses (+) indicates how helpful each test is in assessing the index parameter; while a minus sign (-) means not helpful. ATTR-CA = amyloid transthyretin cardiac amyloidosis; CCT = cardiac CT; CMP = cardiomyopathy; CMR = cardiac magnetic resonance; FDG = fluorodeoxyglucose; SPECT = single photon emission CT; TTE = transthoracic echocardiography. Adapted from: Mitropoulou et al. 2020.¹²⁰ Reproduced from Frontiers Media under a Creative Commons CC-BY licence.

Echocardiography

TTE is the first-line imaging modality and is of unquestionable value in the diagnosis and characterisation of CMPs, as it can identify both structural and functional abnormalities. The main strengths of TTE are availability, low cost, non-invasiveness and possibility of serial testing; possible drawbacks are the reliance on the operator’s experience and the acoustic window, as well as the inter- and intra-observer variability.

Conventional Echocardiography

Conventional echocardiography is an essential tool to characterise LV geometry and function in dilated cardiomyopathy (DCM), and the response to pharmacological and non-pharmacological interventions in terms of reverse remodelling. In hypertrophic cardiomyopathy (HCM), M-mode imaging can identify the systolic anterior motion of the mitral valve, a common, though non-specific, feature, and a determinant of LV outflow tract obstruction (LVOTO).⁴⁻⁶ Continuous wave (CW) Doppler is used to quantify the severity of LVOTO in HCM: the Doppler envelope appears as a “dagger-shaped” and late-peaking curve.⁵ In obstructive HCM, the peak intraventricular gradient is >30 mmHg at rest or after provocative manoeuvres.⁷ Dynamic LVOTO is also identifiable in the acute phase of takotsubo syndrome (intraventricular gradient >25 mmHg), as a result of basal hypercontractility in the LV cavity with an asymmetrical and hypertrophic interventricular septum.⁸ Pulsed wave (PW) Doppler can be used in HCM patients to sample the left anterior descending artery, leading to the frequent finding of a reduced coronary flow reserve (CFR).⁹ Further, abnormal tissue Doppler imaging (TDI) data, such as lateral s’ <13 cm/s and reduced e’ velocities, can be suggestive of an early pre-hypertrophic phenotype.⁷ In restrictive cardiomyopathy (RCM), the change of E/A ratio during the Valsalva manoeuvre is used to define the restrictive filling as reversible (>0.5) or fixed (<0.5, a more severe form).^{10,11} The discrepancy between LV mass and ECG voltages is an important clue to the diagnosis of CA (Figure 1). 2D echocardiography is also useful in arrhythmogenic cardiomyopathy (ACM), as it allows the study of right ventricular (RV) motion and the measurement of RV outflow tract diameter and right ventricle longitudinal systolic function and fractional area change.^{12,13} Contrast agents can be used in rest and stress echocardiography to improve image quality (especially in patients with suboptimal image quality).¹⁴⁻¹⁶

3D Echocardiography

3D echocardiography provides real-time images of the heart in motion that can be displayed at full or cropped volume, allows a more accurate study of cardiac geometry (LV and RV volumes, LV mass) and function (LV and RV ejection fraction, LV regional wall motion, dyssynchrony, and dyssynchrony index). Measurements of linear dimensions and areas can be based on 3D-guided 2D, which ensures higher accuracy than 2D measurements, or on volumetric rendered images that highly depend on image processing.⁷

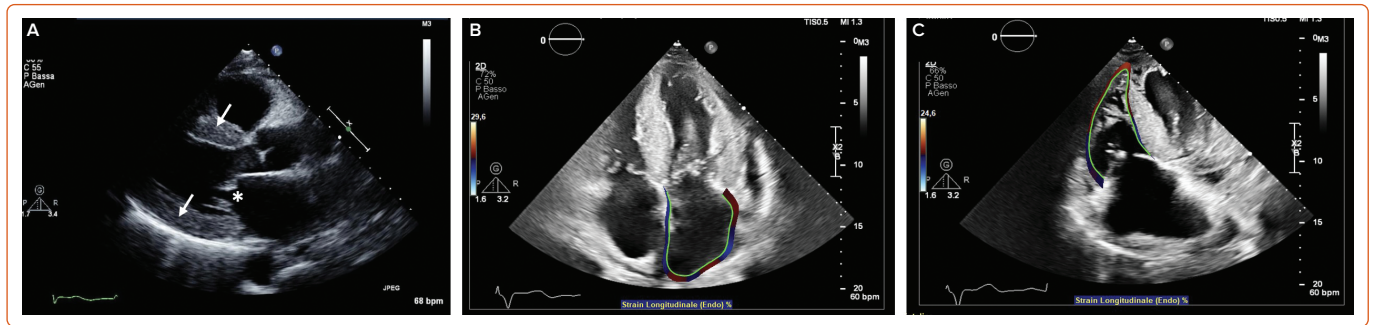
Speckle Tracking Echocardiography

Speckle tracking echocardiography (STE) enables the calculation of motion, velocity, strain and strain rate by identifying a specific image feature, following it frame after frame, and analysing its displacement over time. Good image quality is necessary for STE.⁷ Global longitudinal strain (GLS) is one of the most studied parameters to detect preclinical disease, especially in DCM.¹⁷ Studies on HCM have focused on LA peak strain during the reservoir phase, corresponding to LV systole, while in ACM RV GLS can be calculated by averaging RV peak systolic longitudinal strain values from six RV segments.^{12,18} Conversely, RV free wall longitudinal strain is to be preferred to RV GLS in takotsubo syndrome.¹⁹ In patients with suspected CA, peak LA longitudinal strain and peak atrial contraction strain have independent diagnostic value (Figure 1).²⁰ LV and RV strain, as well as LA enlargement, RV dilatation and RV contractile dysfunction, are important prognostic markers in DCM.⁷ Longitudinal myocardial function can be studied also in cardiac sarcoidosis with 2D STE or TDI-derived strain, allowing the identification of the disease at early stages, when other 2D echo features may be absent.²¹

Stress Echocardiography

Stress echocardiography dynamically evaluates myocardial structure and function under a stress condition induced by physical exercise (using a treadmill or a bicycle) or a pharmacological agent (inotrope or vasodilator). Images are acquired at baseline, at a low workload and at peak exercise.⁷ Myocardial contractile reserve, studied with stress echocardiography, helps distinguish ischaemic from non-ischaemic disease and holds prognostic importance.^{22,23} Moreover, a limited coronary flow and a reduced or absent contractile reserve are often present in subclinical

Figure 1: Echocardiography in Cardiac Amyloidosis



A: Parasternal long axis view showing increased left ventricular wall thickness (arrows) and thickened mitral leaflets (asterisk) in amyloid light-chain amyloidosis; B: Apical four-chamber view showing left atrial strain in transthyretin amyloidosis (ATTR); C: Right ventricle global longitudinal strain in ATTR.

CMPs.^{24–26} Exercise echocardiography is used to quantify mitral regurgitation and to study inducible LVOTO (which is typically increased at the beginning of the recovery phase) in HCM patients.²⁴

Cardiac Magnetic Resonance

CMR is a multi-parametric, highly reproducible, non-invasive imaging technique with a relatively high spatial, temporal and contrast resolution, which has become an essential tool for the evaluation of CMPs. Indeed, CMR allows not only the quantification of biventricular volumes, mass, wall thickness, systolic- and diastolic function, intra- and extracardiac flows, but also the detection of myocardial oedema, fibrosis, and the accumulation of other intra/extracellular substances (such as fat, iron, or amyloid), thus providing unique information for disease characterisation.^{27,28} It has only a few contraindications, mostly related to MR-unsafe metal implants, severe renal dysfunction (which limits the use of several gadolinium-based contrast agents), patient discomfort (claustrophobia), tachyarrhythmias or poor breath-holding ability (which might significantly degrade image quality).²⁹

In patients with non-ischemic DCM, CMR is the gold standard technique for the quantification of biventricular volumes, mass, and EF with cine steady-state free-precession (SSFP) sequences, and for the assessment of myocardial fibrosis with late gadolinium enhancement (LGE) sequences.³⁰ LGE can be found in about 30–50% of DCM patients, typically in a patchy, midwall or subepicardial distribution (Figure 2). Since the first study by Assomull et al. in 2006, midwall fibrosis detected by LGE has emerged as a predictor of adverse prognosis, including all-cause and cardiovascular mortality, sudden cardiac death (SCD), appropriate ICD therapy and ventricular arrhythmias (VA), independently from left ventricular ejection fraction (LVEF).^{31–33} Interestingly, while the relationship between LVEF and VA or SCD is weak in DCM patients, a strong, significant association has been demonstrated between LGE and VA or SCD, even in patients with LVEF >35%. Different LGE location, pattern or extent have different prognostic impacts, although further larger investigations are needed.^{34,35} The absence of LGE predicts the occurrence of reverse remodelling, while the presence and transmural pattern of LGE in the LV lateral wall predicts a poor response to cardiac resynchronisation therapy (CRT).^{36–39} Native myocardial T1 and extracellular volume (ECV) mapping track myocardial fibrosis and interstitial remodelling, and have recently emerged as independent markers of poor outcome.^{40–42} Recently, GLS measured by feature-tracking analysis of cine SSFP images was found to correlate better than LVEF and B-type natriuretic peptide with the composite outcome of cardiac death, heart transplantation and appropriate ICD shock.⁴³ CMR plays a crucial role also in the detection of LV noncompaction (LVNC), whose diagnosis is particularly challenging,

especially due to the overlap with other CMPs and normal LV trabeculation. Besides several geometric diagnostic criteria with limited diagnostic and prognostic utility, the most powerful prognostic parameters in LVNC are the presence of LV systolic dysfunction and LGE.^{44–48}

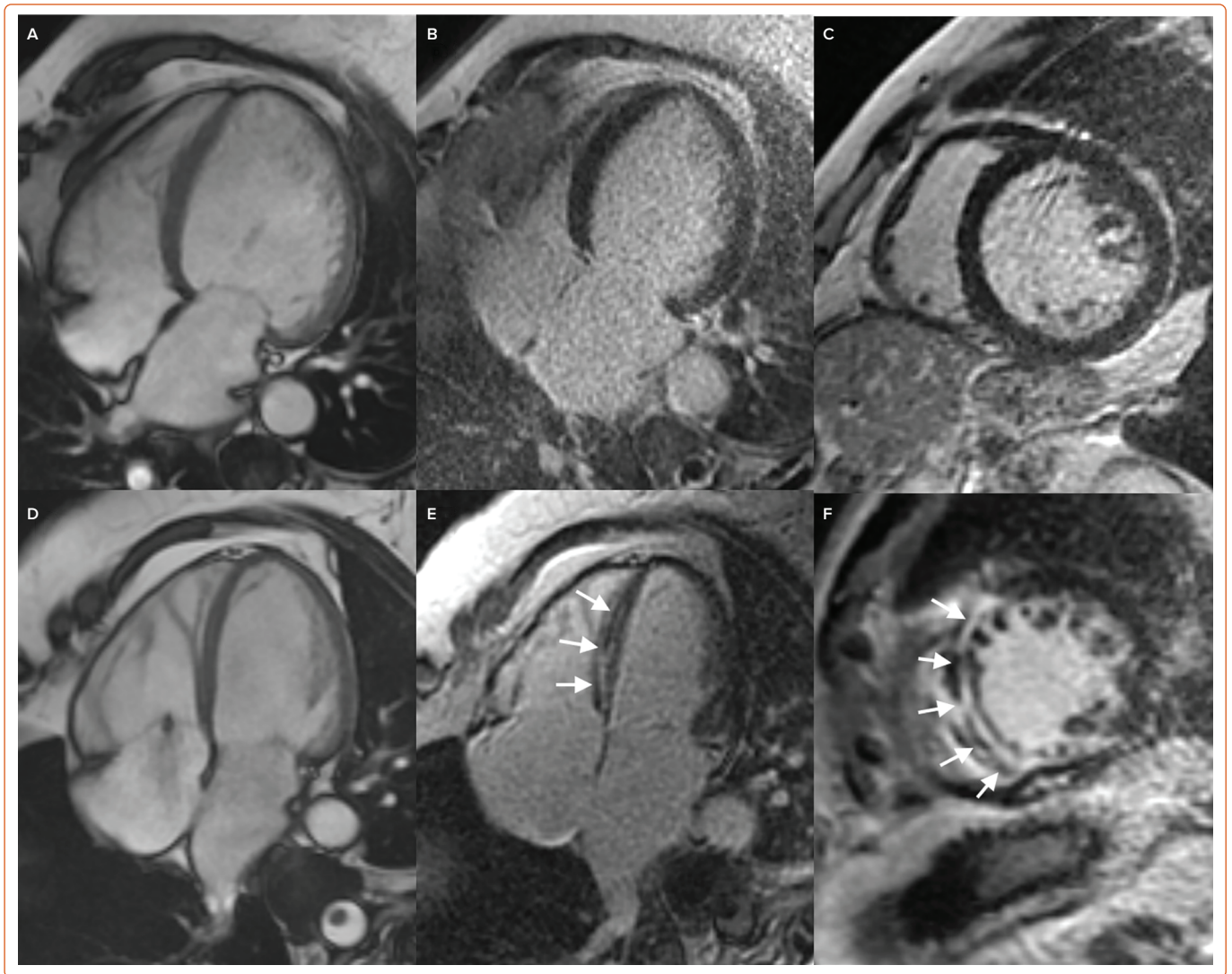
In patients with HCM, CMR allows the morphological assessment of cardiac chambers, including unusual patterns of hypertrophy (lateral, apical or RV distribution), myocardial crypts, papillary muscle abnormalities, elongated mitral valve leaflets and apical aneurysms, which are not always easily visualised by echocardiography.^{49–52} Myocardial fibrosis detected by LGE imaging is a common finding in HCM, occurring in up to 80% of patients (Figure 3), so that only LGE extent is predictive of outcome: an LGE threshold of 10–15% of the LV mass identifies patients at high risk of VA, even in the absence of other major risk factors, and has been listed among the criteria to be considered for the selection of patients to be referred for ICD in the recently updated American Heart Association/American College of Cardiology (AHA/ACC) guidelines.^{53–57} Even scar heterogeneity (expressed as ‘dispersion map of LGE’), scar channels (assessed with an advanced post-processing analysis to differentiate the scar core and the border zone of LGE images), longitudinal strain, myocardial oedema (assessed through T2-weighted imaging), native T1 and ECV mapping are emerging as prognostic markers in HCM patients.^{58–64}

CMR is of utmost importance for the differential diagnosis of hypertrophic phenocopies. In particular, CA is characterised by diffuse subendocardial-to-transmural LGE with variable biventricular and biatrial involvement, which tracks amyloid deposition and patient prognosis: while only subtle LGE areas might be present in the very early disease stages, LGE imaging can be challenging in advanced stages, due to the diffuse nature of LGE and to the equalisation of myocardial and blood pool nulling point.⁶⁵ An increased native T1 demonstrated high diagnostic accuracy in patients with suspected CA, but ECV represents the best parameter to assess amyloid burden, patient outcome and response to treatment.^{66–71}

CMR holds strong potential for diagnostic, prognosis and therapeutic monitoring in Anderson-Fabry disease (AFD), particularly because intracellular glycosphingolipids accumulation causes a shortening of native T1, while ECV is normal compared to other CMPs characterised by interstitial infiltration.⁷²

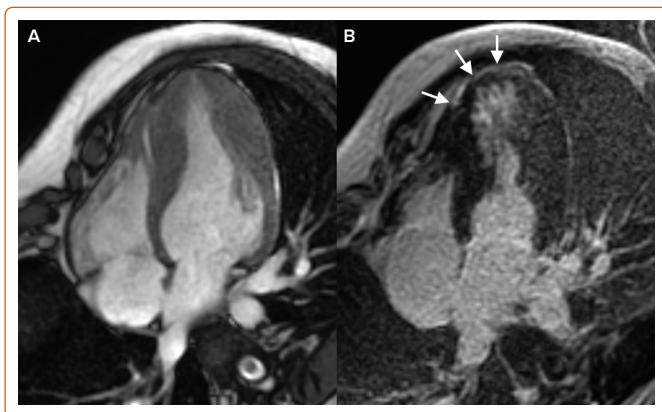
CMR represents an essential tool for the diagnosis and risk stratification of iron overload CMPs, including genetic haemochromatosis and hereditary anaemias: myocardial iron deposits reduce both T2* and native T1 relaxation times, thus allowing an accurate non-invasive diagnosis of cardiac siderosis and treatment monitoring.^{73,74}

Figure 2: Cardiac Magnetic Resonance in Dilated Cardiomyopathy Left Ventricular Dilation in a Patient with Dilated Cardiomyopathy



A: Four-chamber steady-state free-precession diastolic frame, without late gadolinium enhancement; B: Four chamber; C: Short axis view. A similar left ventricular dilation in a different dilated cardiomyopathy patient; D: Four-chamber steady-state free-precession diastolic frame, associated with midwall late gadolinium enhancement in the interventricular septum; E: Four chamber; F: Short axis view (white arrows).

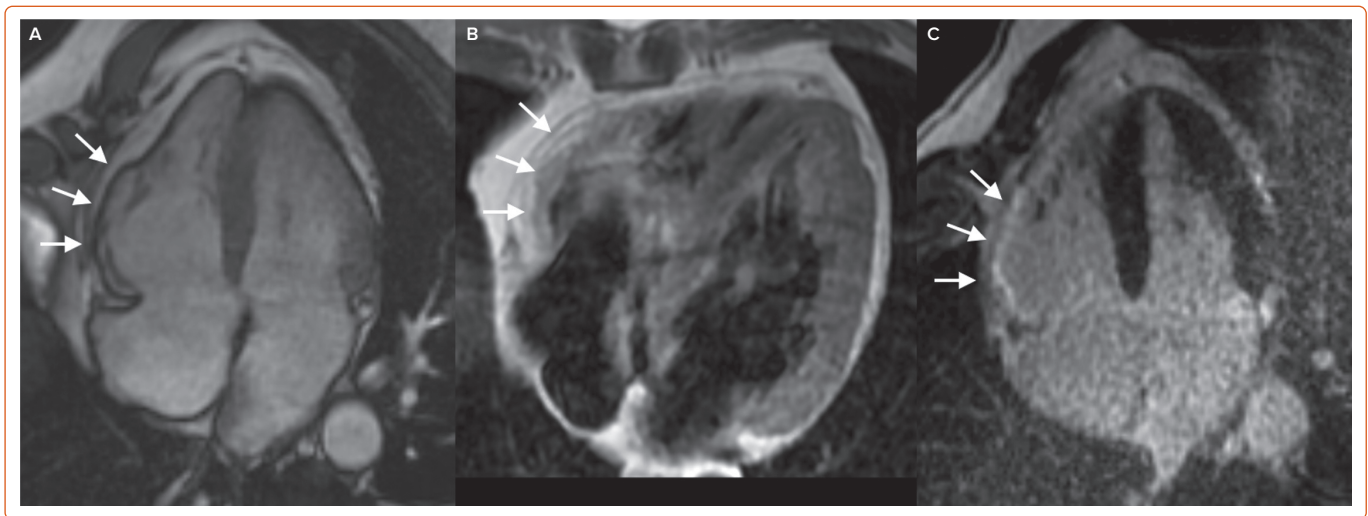
Figure 3: Cardiac Magnetic Resonance in Hypertrophic Cardiomyopathy Disproportionate Apical Hypertrophy in a Patient with Hypertrophic Cardiomyopathy



A: Four-chamber steady-state free-precession diastolic frame, associated with midwall late gadolinium enhancement in the left ventricular apex. B: Four chambers (white arrows).

ACM is a genetically determined heart muscle disease characterised by myocardial fibro-fatty replacement with variable RV and LV involvement, clinically associated with malignant ventricular arrhythmias and SCD.⁷⁵ CMR has always been regarded as a tool for the non-invasive detection of major morpho-functional abnormalities (biventricular dilation, dysfunction and regional wall motion abnormalities) (Figure 4). In the recently published Padua criteria, CMR has gained further importance, with the inclusion of LGE as a major structural criterion besides endomyocardial biopsy.⁷⁶ The presence of circumferential LV subepicardial LGE in short axis view (ring pattern) has been consistently reported in left-dominant forms with a specific genotype.⁷⁷ Similarly to DCM, LV LGE identifies patients with a high arrhythmic risk who are candidates to ICD implantation regardless of the severity of systolic dysfunction.⁷⁸ CMR can also detect myocardial fatty infiltration as hyperintense areas on T1- or proton density (PD)-weighted images, or as India ink artefacts at conventional cine-SSFP images, which nonetheless have limited sensitivity and specificity in the context of a low spatial resolution.^{79,80} T2-weighted images might allow the depiction of myocardial oedema in case of an ACM presentation with chest pain and troponin release, which might be encountered in paediatric

Figure 4: Cardiac Magnetic Resonance in Arrhythmogenic Cardiomyopathy Right Ventricular Arrhythmogenic Cardiomyopathy, Manifesting with Right Ventricular Free Wall Hypo/Akinesia



A: Four-chamber steady-state free-precession diastolic frame. B: Subepicardial fatty infiltration at black-blood proton-density spin-echo imaging. C: Late gadolinium enhancement.

patients and carriers of *DSP* (desmoplakin) gene mutations with a clinical presentation similar to a recurrence of myocarditis.^{81,82}

Nuclear Medicine

Nuclear medicine offers imaging tools to evaluate myocardial perfusion, innervation and metabolism induced by inflammatory processes as in myocarditis and cardiac sarcoidosis, or in CA. In the last decade, the use of specific single-photon emission CT (SPECT) radiopharmaceuticals has allowed the identification of the presence of ATTR-CA, while the use of new PET radiopharmaceuticals could help to achieve an early diagnosis of immunoglobulin light-chain (AL) CA without the need for biopsy confirmation.

Perfusion and Innervation SPECT Tracers

SPECT with tracers such as ²⁰¹Tl, sestamibi or tetrofosmin labelled with ^{99m}Tc allows the exclusion of the presence of ischaemia, particularly in patients with HCM who present with chest pain or who have LV systolic dysfunction. Using dedicated software, it is possible to estimate the systolic and diastolic function of the LV from a myocardial perfusion study.^{83,84} In cardiac sarcoidosis, the assessment of LV contraction dyssynchrony by myocardial perfusion-gated SPECT can be useful for prognostic stratification; furthermore, the assessment of perfusion recovery after corticosteroid therapy seems to be associated with a lower risk of major adverse cardiac events.^{85,86}

SPECT with ¹²³I-labelled metaiodobenzylguanidine (MIBG) allows the evaluation of the integrity of myocardial adrenergic innervation. In AFD, the extent of impairment of adrenergic innervation correlates with the degree of fibrosis, but autonomic dysfunction appears to precede myocardial fibrosis, so the innervation scintigraphy could allow an earlier diagnosis of this disease.⁸⁷ A reduction in the density of adrenergic endings has also been reported in CA, probably as a consequence of the toxic effect of the amyloid fibrils.^{88,89} The use of ¹²³I-MIBG for the evaluation of adrenergic damage has also been described in patients with cardiac sarcoidosis, but it is not routinely adopted.^{90,91}

PET Tracers Assessing Myocardial Inflammation

¹⁸F-labelled fluorodeoxyglucose (FDG) is the main radiopharmaceutical used in PET. Although its main use is oncological, it is not tumour-specific, and it allows the visualisation of areas of leukocyte infiltration during

inflammatory processes. The degree of glucose uptake in the vital myocardium correlates directly with the circulating levels of insulin and inversely with the level of circulating free fatty acids, while the degree of glucose metabolism of the inflammatory tissue is relatively independent of insulin. For this reason, the use of ¹⁸F-FDG for the study of myocarditis requires an adequate dietary preparation that suppresses the myocardial glucose uptake.⁹²⁻⁹⁴ PET with ¹⁸F-FDG can be used to characterise the inflammatory response after acute myocardial infarction, to assess the extent of the disease and the response to therapy in the case of myocarditis and in sarcoidosis.⁹⁵⁻⁹⁸ Lymphocytes involved in the granulomatous process of sarcoidosis express membrane receptors for somatostatin; new PET radiopharmaceuticals with an affinity for somatostatin receptors, such as the peptides DOTATOC, DOTATATE and DOTANOC labelled with ⁶⁸Ga, have been shown to have a greater diagnostic accuracy than ¹⁸F-FDG for cardiac sarcoidosis.⁹⁹

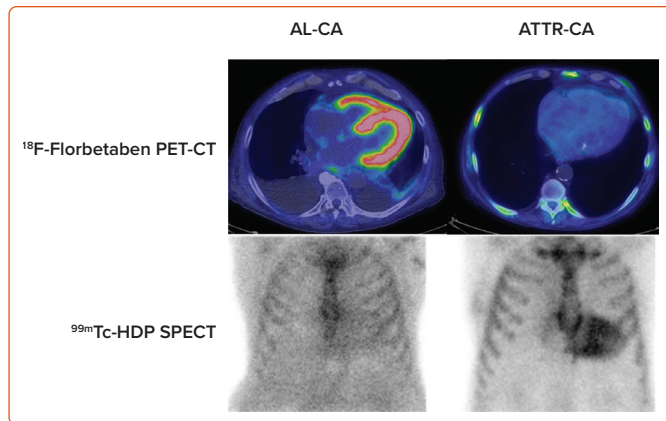
Nuclear Medicine in Cardiac Amyloidosis

Some SPECT tracers originally developed to study bone metabolism and labelled with ^{99m}Tc have been successfully used to identify ATTR-CA. ^{99m}Tc-3,3-diphosphono-1,2-propanodicarboxylic acid (DPD) cardiac uptake in patients with ATTR-CA has been known since the 1970s; thanks to the evidence collected in the last 15 years, bone tracer scintigraphy has been a fundamental tool in the diagnostic path of patients with suspected ATTR-CA.¹⁰⁰ ¹⁸F-NaF is a PET radiopharmaceutical for bone imaging that also accumulates in myocardial ATTR deposits.^{101,102} However, a lower sensitivity of PET compared to scintigraphy has been reported.^{103,104} In the last decade, PET radiopharmaceuticals developed for brain amyloid substance have shown binding affinity also for myocardial amyloid, both in the context of a systemic amyloidosis with cardiac involvement and in the case of isolated CA.¹⁰⁵⁻¹¹⁰ The most promising of these tracers is ¹⁸F-florbetaben, which has proven able not only to identify CA, but also to discriminate between AL-CA and other mimicking conditions and to evaluate the response to therapy (Figure 5).^{111,112}

Cardiac CT

The latest generation of CCT equipment, with the implementation of temporal resolution, the use of lower kV values, high volume coverage, iterative reconstruction algorithms and low radiation exposure, allows the assessment of ventricular and atrial size, morphology, function, density,

Figure 5: Nuclear Medicine in Cardiac Amyloidosis Scans from ^{18}F -Florbetaben PET and from $^{99\text{m}}\text{Tc}$ -HDP Scintigraphy in a Patient with Light Chain Cardiac Amyloidosis



Myocardial uptake at PET imaging and negative bone-tracer scintigraphy, and in a patient with transthyretin cardiac amyloidosis, with negative PET scan and myocardial uptake at bone-tracer scintigraphy. AL-CA = immunoglobulin light-chain cardiac amyloidosis. ATTR-CA = amyloid transthyretin cardiac amyloidosis.

first pass perfusion defects and delayed-enhancement pattern in sub-millimetric multiplanar reconstructions with a short acquisition time.¹¹³ In the setting of CMPs, pre-contrast CCT can easily depict myocardial areas with adipose density as well as calcifications. After contrast enhancement, in addition to providing information on the causes of ischaemia and on the risk of major cardiac events, CCT can qualitatively and quantitatively assess myocardial perfusion and the presence of myocardial muscle alterations, discriminating between ischaemic and non-ischaemic aetiology, disclosing myocardial phenotype, the presence of fat, as well as complications such as intracavitary thrombosis.^{114,115} CCT may therefore be considered as an option in patients with contraindications to CMR or when coronary artery disease must be ruled out.¹¹⁶ Next challenges will concern the evaluation of myocardial metabolism with CCT photon counting and the assessment of myocardial oedema and fibrosis.^{117,118}

Multimodality Imaging and Integration with Circulating Biomarkers

The integration of different imaging techniques may help overcome the different limitations and weaknesses of single techniques.^{17,119} For example, echocardiographic findings may be non-specific, therefore, have a limited role in identifying the underlying aetiology.¹¹⁹ CMR is generally performed after echocardiography and has a primary role in assessing the aetiology of CMPs.¹²⁰ CMR findings, namely LGE and parametric imaging (T1 and T2 values), allow an accurate characterisation of myocardial tissue in terms of fibrosis, scar, inflammation, oedema, or infiltration.^{119,120} CCT is highly valuable to exclude significant epicardial coronary artery disease in DCM.¹⁷ Additionally, the good spatial resolution and ease of navigation make cardiac CCT an option in the presence of suboptimal echocardiographic findings and contraindications to CMR.¹⁷

The integration of imaging with circulating biomarkers allows an even more accurate characterisation of the different types of CMPs.¹²¹ For example, although the role of nuclear imaging is generally limited in the evaluation of patients with suspected CMPs, ATTR-CA is diagnosed with a 100% specificity in the presence of a positive bone scintigraphy combined with the absence of a monoclonal protein or abnormal light chains in blood samples.¹²² In addition, specific imaging markers provide additional information to biomarkers and refine risk prediction in AL-CA.¹²³

Further research is required to integrate imaging findings from different techniques with clinical data and circulating biomarkers to create a multifactorial algorithm for the diagnosis and prognostic assessment, as well as for the individualisation of therapy in each specific CMP.¹¹⁹

Perspectives

The growing body of knowledge on the pathophysiology and natural history of CMPs, and the availability of disease-modifying therapies for some conditions have made early diagnosis more crucial than ever. However, some CMPs may show milder phenotypes in early disease stages, which can overlap between different diseases or even physiological conditions. Emblematic cases are represented by DCM versus ACM with prevalent LV involvement, or HCM versus athlete's heart.^{17,124} The integration of additional information from different imaging modalities can maximise the diagnostic performance.¹⁷ For inherited CMPs with adolescent-onset, such as HCM and some forms of ACM, early diagnosis presents additional challenges, particularly for family screening. First, the diagnostic criteria have been mostly validated on adult subjects with well-differentiated phenotypes, therefore, their diagnostic performance at a younger age may be lower.¹²⁵ Second, echocardiography is the preferred tool for screening, but is unable to identify subtler structural abnormalities, so it currently remains to be defined which methods and timing are the most appropriate for family screening of inherited CMPs. For example, the 2014 ESC guidelines on the diagnosis and management of HCM recommend clinical evaluation with ECG and echocardiography and long-term follow-up in first-degree relatives who have the same defined pathological mutation as the proband; when no definite genetic mutation is identified in the proband, ECG and echocardiography should be considered in first-degree adult relatives and repeated every 2–5 years (or 6–12 months if nondiagnostic abnormalities are present).¹²⁶ Similar recommendations are provided by the 2020 AHA/ACC Guidelines, which also mention the possibility of employing CMR for family screening when echocardiography is inconclusive.⁵⁷ As for ACM, the 2019 Heart Rhythm Society (HRS) expert consensus statement recommends clinical evaluation by ECG and cardiac imaging every 1–3 years starting at 10–12 years of age in first-degree relatives. However, the precise imaging technique to be employed is not specified.¹²⁷

Another future perspective is the validation of new diagnostic methods and their integration into the diagnostic flow charts of CMPs. CMR mapping techniques have proven to be very reliable in supporting the diagnosis of CA and predicting prognosis, yet CMR currently has a secondary role in the diagnostic flow chart of CA proposed by the ESC.² In many cases of suspected CMP, endomyocardial biopsy is still crucial.¹²⁸ However, in the near future, new imaging tools might limit the need for endomyocardial biopsy in specific cases. For example, recent studies have shown that delayed cardiac uptake of ^{18}F -florbetaben on PET/CT imaging is able to accurately discriminate AL-CA from either ATTR-CA or other phenocopies.¹¹¹

Besides diagnosis, imaging tools can be used to highlight collateral structural abnormalities of some CMPs that might have clinical relevance. For example, it has been demonstrated that some forms of ACM, such as those caused by *DSP* mutations, can have a clinical course that passes through “hot phases” characterised by myocardial inflammation and the release of biomarkers of myocardial damage, which sometimes are misdiagnosed as acute myocarditis.⁸¹ These phases hold prognostic significance and can be identified both by CMR as the presence of oedema T2-weighted sequences and by ^{18}F -FDG PET.^{124,129} Myocardial

oedema detected through CMR can also be a hallmark of cardiac remodelling in HCM, and is associated with more advanced disease and increased arrhythmic load.⁶¹

Finally, the role of advanced imaging modalities in monitoring the response to therapy remains to be defined. One study on patients with ATTR-CA has demonstrated that serial ECV quantification by CMR can be used to monitor the effectiveness of reducing the cardiac amyloid burden by patisiran, a small interfering RNA able to knock down the expression of transthyretin in the liver.⁷¹ Similarly, it has been recently demonstrated that ECV quantification by CMR can be used to monitor cardiac amyloid regression following chemotherapy in AL amyloidosis. Notably, a deep haematologic response is not sufficient per se to grant cardiac amyloid regression, while changes in ECV over time independently predict prognosis, making it a unique marker of treatment response.¹³⁰

Conclusion

Recent advances in cardiac imaging and its increased accessibility allow a precise assessment of ventricular dimension and function, as well as a non-invasive tissue characterisation of the myocardium. However, the growing knowledge from imaging studies should always be interpreted based on all clinical elements (i.e. clinical assessment, electrocardiographic findings, biomarkers, genetic and functional assessment). While echocardiography remains the first-line imaging tool for the management of patients with CMP and can be implemented with advanced analyses (e.g. STE, stress echocardiography, contrast-enhanced echocardiography), CMR represents the gold standard technique for myocardial anatomy and tissue characterisation, including novel tools (e.g. T1/T2/T2*/ECV mapping, quantitative perfusion, diffusion tensor imaging and feature tracking). An integrated clinical and imaging approach seems essential to characterise the CMP phenotype and identify the underlying aetiologies, to predict disease prognosis and to ensure a tailored therapeutic management. □

1. Elliott P, Andersson B, Arbustini E, et al. Classification of the cardiomyopathies: a position statement from the European Society of Cardiology Working Group on Myocardial and Pericardial Diseases. *Eur Heart J* 2008;29:270–6. <https://doi.org/10.1093/eurheartj/ehm342>; PMID: 17916581.
2. Garcia-Pavia P, Rapezzi C, Adler Y, et al. Diagnosis and treatment of cardiac amyloidosis. A position statement of the European Society of Cardiology Working Group on Myocardial and Pericardial Diseases. *Eur J Heart Fail* 2021;23:512–26. <https://doi.org/10.1002/ehfj.2140>; PMID: 33826207.
3. Casas G, Rodríguez-Palomares JF. Multimodality cardiac imaging in cardiomyopathies: from diagnosis to prognosis. *J Clin Med* 2022;11:578. <https://doi.org/10.3390/jcm11030578>; PMID: 35160031.
4. Rankin K, Thampinathan B, Thavendiranathan P. Imaging-specific cardiomyopathies a practical guide. *Heart Fail Clin* 2019;15:275–95. <https://doi.org/10.1016/j.hfc.2018.12.007>; PMID: 30832818.
5. Cardim N, Galderisi M, Edvardsen T, et al. Role of multimodality cardiac imaging in the management of patients with hypertrophic cardiomyopathy: an expert consensus of the European Association of Cardiovascular Imaging endorsed by the Saudi Heart Association. *Eur Heart J Cardiovasc Imaging* 2015;16:280. <https://doi.org/10.1093/ehjci/jeu291>; PMID: 25650407.
6. Nagueh SF, Bierig SM, Budoff MJ, et al. American Society of Echocardiography clinical recommendations for multimodality cardiovascular imaging of patients with hypertrophic cardiomyopathy. *J Am Soc Echocardiogr* 2022;35:533–69. <https://doi.org/10.1016/j.echo.2022.03.012>; PMID: 35659037.
7. Lancellotti P, Cosyns B, eds. *The EACVI echo handbook*. Oxford: Oxford University Press, 2016.
8. Chockalingam A, Xie GY, Dellspinger KC. Echocardiography in stress cardiomyopathy and acute LVOT obstruction. *Int J Cardiovasc Imaging* 2010;26:527–35. <https://doi.org/10.1007/s10584-010-9590-7>; PMID: 20119847.
9. Cortigiani L, Rigo F, Gherardi S, et al. Prognostic implications of coronary flow reserve on left anterior descending coronary artery in hypertrophic cardiomyopathy. *Am J Cardiol* 2008;102:1718–23. <https://doi.org/10.1016/j.amjcard.2008.08.023>; PMID: 19064030.
10. Habib G, Bucciarelli-Ducci C, Caforio ALP, et al. Multimodality imaging in restrictive cardiomyopathies: an EACVI expert consensus document in collaboration with the "Working Group on Myocardial and Pericardial Diseases" of the European Society of Cardiology endorsed by the Indian Academy of Echocardiography. *Eur Heart J Cardiovasc Imaging* 2017;18:1090–121. <https://doi.org/10.1093/ehjci/jeu034>; PMID: 28510718.
11. Nagueh SF, Smiseth OA, Appleton CP, et al. Recommendations for the evaluation of left ventricular diastolic function by echocardiography: an update from the American Society of Echocardiography and the European Association of Cardiovascular Imaging. *J Am Soc Echocardiogr* 2016;29:277–314. <https://doi.org/10.1016/j.echo.2016.01.011>; PMID: 27037982.
12. Haugaa KH, Basso C, Badano LP, et al. Comprehensive multi-modality imaging approach in arrhythmogenic cardiomyopathy – an expert consensus document of the European Association of Cardiovascular Imaging. *Eur Heart J Cardiovasc Imaging* 2017;18:237–53. <https://doi.org/10.1093/ehjci/jev229>; PMID: 28069601.
13. Marcus FI, McKenna WJ, Sherrill D, et al. Diagnosis of arrhythmogenic right ventricular cardiomyopathy/dysplasia: proposed modification of the Task Force Criteria. *Eur Heart J* 2010;31:806–14. <https://doi.org/10.1093/eurheartj/ehq025>; PMID: 20172912.
14. Mansencal N, Pellerin D, Lamar A, et al. Diagnostic value of contrast echocardiography in Tako-Tsubo cardiomyopathy. *Arch Cardiovasc Dis* 2010;103:447–53. <https://doi.org/10.1016/j.acvd.2010.08.001>; PMID: 21074123.
15. Nunes MCP, Badano LP, Marin-Neto JA, et al. Multimodality imaging evaluation of Chagas disease: an expert consensus of Brazilian Cardiovascular Imaging Department (DIC) and the European Association of Cardiovascular Imaging (EACVI). *Eur Heart J Cardiovasc Imaging* 2018;19:459–460n. <https://doi.org/10.1093/ehjci/jez154>; PMID: 29029074.
16. Viotti RJ, Vigliano C, Laucella S, et al. Value of echocardiography for diagnosis and prognosis of chronic Chagas disease cardiomyopathy without heart failure. *Heart* 2004;90:655–60. <https://doi.org/10.1136/hrt.2003.018960>; PMID: 15145872.
17. Donal E, Delgado V, Bucciarelli-Ducci C, et al. Multimodality imaging in the diagnosis, risk stratification, and management of patients with dilated cardiomyopathies: an expert consensus document from the European Association of Cardiovascular Imaging. *Eur Heart J Cardiovasc Imaging* 2019;20:1075–93. <https://doi.org/10.1093/ehjci/jez178>; PMID: 31504368.
18. Paraskevaidis IA, Panou F, Papadopoulos C, et al. Evaluation of left atrial longitudinal function in patients with hypertrophic cardiomyopathy: a tissue Doppler imaging and two-dimensional strain study. *Heart* 2009;95:483–9. <https://doi.org/10.1136/hrt.2008.146548>; PMID: 18765436.
19. Heggemann F, Hamm K, Brade J, et al. Right ventricular function quantification in takotsubo cardiomyopathy using two-dimensional strain echocardiography. *PLoS One* 2014;9:e103717. <https://doi.org/10.1371/journal.pone.0103717>; PMID: 25089702.
20. Aimo A, Fabiani I, Gianmoni A, et al. Multi-chamber speckle tracking imaging and diagnostic value of left atrial strain in cardiac amyloidosis. *Eur Heart J Cardiovasc Imaging* 2022;24:130–41. <https://doi.org/10.1093/ehjci/jeac057>; PMID: 35292807.
21. A joint procedural position statement on imaging in cardiac sarcoidosis: from the Cardiovascular and Inflammation & Infection Committees of the European Association of Nuclear Medicine. *Eur Heart J Cardiovasc Imaging* 2017;18:1073–89. <https://doi.org/10.1093/ehjci/jev146>; PMID: 28984894.
22. Sicari R, Nihoyannopoulos P, Evangelista A, et al. Stress echocardiography expert consensus statement – executive summary. *Eur Heart J* 2009;30:278–89. <https://doi.org/10.1093/eurheartj/ehn492>; PMID: 19001473.
23. Pellikka PA, Nagueh SF, Elhendy AA, et al. American Society of Echocardiography recommendations for performance, interpretation, and application of stress echocardiography. *J Am Soc Echocardiogr* 2007;20:1021–41. <https://doi.org/10.1016/j.echo.2007.07.003>; PMID: 17765820.
24. Sicari R, Nihoyannopoulos P, Evangelista A, et al. Stress echocardiography expert consensus statement: European Association of Echocardiography (EAE) (a registered branch of the ESC). *Eur J Echocardiogr* 2008;9:415–37. <https://doi.org/10.1093/ejehocardi/jen175>; PMID: 18579481.
25. Naqvi TZ, Goel RK, Forrester JS, Siegel RJ. Myocardial contractile reserve on dobutamine echocardiography predicts late spontaneous improvement in cardiac function in patients with recent onset idiopathic dilated cardiomyopathy. *J Am Coll Cardiol* 1999;34:1537–44. [https://doi.org/10.1016/s0735-1097\(99\)00371-x](https://doi.org/10.1016/s0735-1097(99)00371-x); PMID: 10551704.
26. Lee JH, Yang DH, Choi WS, et al. Prediction of improvement in cardiac function by high dose dobutamine stress echocardiography in patients with recent onset idiopathic dilated cardiomyopathy. *Int J Cardiol* 2013;167:1649–50. <https://doi.org/10.1016/j.ijcard.2012.11.021>; PMID: 23312406.
27. Grigoratos C, Todiore G, Barison A, Aquaro GD. The role of MRI in prognostic stratification of cardiomyopathies. *Curr Cardiol Rep* 2020;22:61. <https://doi.org/10.1007/s11886-020-01311-3>; PMID: 32562090.
28. Merlo M, Gagno G, Baritussio A, et al. Clinical application of CMR in cardiomyopathies: evolving concepts and techniques: a position paper of myocardial and pericardial diseases and cardiac magnetic resonance working groups of Italian society of cardiology. *Heart Fail Rev* 2023;28:77–95. <https://doi.org/10.1007/s10741-022-10235-9>; PMID: 35536402.
29. Barison A, Baritussio A, Cipriani A, et al. Cardiovascular magnetic resonance: what clinicians should know about safety and contraindications. *Int J Cardiol* 2021;331:322–8. <https://doi.org/10.1016/j.ijcard.2021.02.003>; PMID: 33571560.
30. Barison A, Grigoratos C, Todiore G, Aquaro GD. Myocardial interstitial remodelling in non-ischaemic dilated cardiomyopathy: insights from cardiovascular magnetic resonance. *Heart Fail Rev* 2015;20:731–49. <https://doi.org/10.1007/s10741-015-9509-4>; PMID: 26423909.
31. Assomull RG, Prasad SK, Lyne J, et al. Cardiovascular magnetic resonance, fibrosis, and prognosis in dilated cardiomyopathy. *J Am Coll Cardiol* 2006;48:1977–85. <https://doi.org/10.1016/j.jacc.2006.07.049>; PMID: 17112987.
32. Di Marco A, Anguera I, Schmitt M, et al. Late gadolinium enhancement and the risk for ventricular arrhythmias or sudden death in dilated cardiomyopathy. *JACC Heart Fail* 2017;5:28–38. <https://doi.org/10.1016/j.jchf.2016.09.017>; PMID: 28017348.
33. Guaricci AI, Masci PG, Muscogiuri G, et al. Cardiac magnetic resonance for prophylactic implantable-cardioverter defibrillator therapy in non-ischaemic dilated cardiomyopathy: an international registry. *Europace* 2021;23:1072–83. <https://doi.org/10.1093/europace/ueaa401>; PMID: 33792661.
34. Halliday BP, Baksi AJ, Gulati A, et al. Outcome in dilated cardiomyopathy related to the extent, location, and pattern of late gadolinium enhancement. *JACC Cardiovasc Imaging* 2019;12:1645–55. <https://doi.org/10.1016/j.jcmg.2018.07.015>; PMID: 30219397.
35. Barison A, Aimo A, Mirizzi G, et al. The extent and location of late gadolinium enhancement predict defibrillator shock and cardiac mortality in patients with non-ischaemic dilated cardiomyopathy. *Int J Cardiol* 2020;307:180–6. <https://doi.org/10.1016/j.ijcard.2020.02.028>; PMID: 32067833.
36. Ikeda Y, Inomata T, Fujita T, et al. Cardiac fibrosis detected by magnetic resonance imaging on predicting time course diversity of left ventricular reverse remodeling in patients with idiopathic dilated cardiomyopathy. *Heart Vessels* 2016;31:1817–25. <https://doi.org/10.1007/s00380-016-0805-2>; PMID: 26843195.

37. Barison A, Aimo A, Ortalda A, et al. Late gadolinium enhancement as a predictor of functional recovery, need for defibrillator implantation and prognosis in non-ischemic dilated cardiomyopathy. *Int J Cardiol* 2018;250:195–200. <https://doi.org/10.1016/j.ijcard.2017.10.043>; PMID: 29107357.
38. Leyva F, Foley PW, Chaili S, et al. Cardiac resynchronization therapy guided by late gadolinium-enhancement cardiovascular magnetic resonance. *J Cardiovasc Magn Reson* 2011;13:29. <https://doi.org/10.1186/1532-429X-13-29>; PMID: 21668964.
39. Taylor RJ, Umar F, Panting JR, et al. Left ventricular lead position, mechanical activation, and myocardial scar in relation to left ventricular reverse remodeling and clinical outcomes after cardiac resynchronization therapy: a feature-tracking and contrast-enhanced cardiovascular magnetic resonance study. *Heart Rhythm* 2016;13:481–9. <https://doi.org/10.1016/j.hrthm.2015.10.024>; PMID: 26498258.
40. Puntmann VO, Carr-White G, Jabour A, et al. T1-mapping and outcome in nonischemic cardiomyopathy: all-cause mortality and heart failure. *JACC Cardiovasc Imaging* 2016;9:40–50. <https://doi.org/10.1016/j.jcmg.2015.12.001>; PMID: 26762873.
41. Barison A, Del Torto A, Chiappino S, et al. Prognostic significance of myocardial extracellular volume fraction in nonischemic dilated cardiomyopathy. *J Cardiovasc Med (Hagerstown)* 2015;16:681–7. <https://doi.org/10.2459/JCM.0000000000000275>; PMID: 26090916.
42. Vita T, Grani C, Abbasi SA, et al. Comparing CMR mapping methods and myocardial patterns toward heart failure outcomes in nonischemic dilated cardiomyopathy. *JACC Cardiovasc Imaging* 2019;12:1659–69. <https://doi.org/10.1016/j.jcmg.2018.08.021>; PMID: 30448130.
43. Buss SJ, Breuninger K, Lehrke S, et al. Assessment of myocardial deformation with cardiac magnetic resonance strain imaging improves risk stratification in patients with dilated cardiomyopathy. *Eur Heart J Cardiovasc Imaging* 2015;16:307–15. <https://doi.org/10.1093/ehjci/jeu181>; PMID: 25246506.
44. Petersen SE, Selvanayagam JB, Wiesmann F, et al. Left ventricular non-compaction: insights from cardiovascular magnetic resonance imaging. *J Am Coll Cardiol* 2005;46:101–5. <https://doi.org/10.1016/j.jacc.2005.03.045>; PMID: 15992642.
45. Jacquier A, Thuny F, Jop B, et al. Measurement of trabeculated left ventricular mass using cardiac magnetic resonance imaging in the diagnosis of left ventricular non-compaction. *Eur Heart J* 2010;31:1098–104. <https://doi.org/10.1093/eurheartj/ehp595>; PMID: 20089517.
46. Grothoff M, Pachowsky M, Hoffmann J, et al. Value of cardiovascular MR in diagnosing left ventricular non-compaction cardiomyopathy and in discriminating between other cardiomyopathies. *Eur Radiol* 2012;22:2699–709. <https://doi.org/10.1007/s00330-012-2554-7>; PMID: 22772366.
47. Grigoratos C, Barison A, Ivanov A, et al. Meta-analysis of the prognostic role of late gadolinium enhancement and global systolic impairment in left ventricular noncompaction. *JACC Cardiovasc Imaging* 2019;12:2141–51. <https://doi.org/10.1016/j.jcmg.2018.12.029>; PMID: 30878415.
48. Macaione F, Meloni A, Positano V, et al. The prognostic role of CMR using global planimetric criteria in patients with excessive left ventricular trabeculation. *Eur Radiol* 2021;31:7553–65. <https://doi.org/10.1007/s00330-021-07875-0>; PMID: 33821336.
49. Maron MS, Rowin EJ, Maron BJ. How to image hypertrophic cardiomyopathy. *Circ Cardiovasc Imaging* 2017;10:e005372. <https://doi.org/10.1161/CIRCIMAGING.116.005372>; PMID: 28701526.
50. Harrigan CJ, Appelbaum E, Maron BJ, et al. Significance of papillary muscle abnormalities identified by cardiovascular magnetic resonance in hypertrophic cardiomyopathy. *Am J Cardiol* 2008;101:668–73. <https://doi.org/10.1016/j.amjcard.2007.10.032>; PMID: 18308018.
51. Captur G, Lopes LR, Mohun TJ, et al. Prediction of sarcomere mutations in subclinical hypertrophic cardiomyopathy. *Circ Cardiovasc Imaging* 2014;7:863–71. <https://doi.org/10.1161/CIRCIMAGING.114.002411>; PMID: 25228707.
52. Reant P, Captur G, Mirabel M, et al. Abnormal septal convexity into the left ventricle occurs in subclinical hypertrophic cardiomyopathy. *J Cardiovasc Magn Reson* 2015;17:64. <https://doi.org/10.1186/s12968-015-0160-y>; PMID: 26219660.
53. Aquaro GD, Masci P, Formisano F, et al. Usefulness of delayed enhancement by magnetic resonance imaging in hypertrophic cardiomyopathy as a marker of disease and its severity. *Am J Cardiol* 2010;105:392–7. <https://doi.org/10.1016/j.amjcard.2009.09.045>; PMID: 20102955.
54. Chan RH, Maron BJ, Olivetto I, et al. Prognostic value of quantitative contrast-enhanced cardiovascular magnetic resonance for the evaluation of sudden death risk in patients with hypertrophic cardiomyopathy. *Circulation* 2014;130:484–95. <https://doi.org/10.1161/CIRCULATIONAHA.113.007094>; PMID: 25092278.
55. Todiére G, Nugara C, Gentile G, et al. Prognostic role of late gadolinium enhancement in patients with hypertrophic cardiomyopathy and low-to-intermediate sudden cardiac death risk score. *Am J Cardiol* 2019;124:1286–92. <https://doi.org/10.1016/j.amjcard.2019.07.023>; PMID: 31447011.
56. Freitas P, Ferreira AM, Artega-Fernández E, et al. The amount of late gadolinium enhancement outperforms current guideline-recommended criteria in the identification of patients with hypertrophic cardiomyopathy at risk of sudden cardiac death. *J Cardiovasc Magn Reson* 2019;21:50. <https://doi.org/10.1186/s12968-019-0561-4>; PMID: 31412875.
57. Ommen SR, Mital S, Burke MA, et al. AHA/ACC guideline for the diagnosis and treatment of patients with hypertrophic cardiomyopathy. *J Am Coll Cardiol* 2020;76:3022–55. <https://doi.org/10.1016/j.jacc.2020.08.044>; PMID: 33229115.
58. Aquaro GD, Grigoratos C, Bracco A, et al. Late gadolinium enhancement–dispersion mapping: a new magnetic resonance imaging technique to assess prognosis in patients with hypertrophic cardiomyopathy and low-intermediate 5-year risk of sudden death. *Circ Cardiovasc Imaging* 2020;13:e010489. <https://doi.org/10.1161/CIRCIMAGING.120.010489>; PMID: 32539460.
59. Sánchez-Somonte P, Quinto L, Garre P, et al. Scar channels in cardiac magnetic resonance to predict appropriate therapies in primary prevention. *Heart Rhythm* 2021;18:1336–43. <https://doi.org/10.1016/j.hrthm.2021.04.017>; PMID: 33892202.
60. Negri F, Musser D, Driussi M, et al. Prognostic role of global longitudinal strain by feature tracking in patients with hypertrophic cardiomyopathy: the STRAIN-HCM study. *Int J Cardiol* 2021;345:61–7. <https://doi.org/10.1016/j.ijcard.2021.10.148>; PMID: 34728259.
61. Todiére G, Piscicella L, Barison A, et al. Abnormal T2-STIR magnetic resonance in hypertrophic cardiomyopathy: a marker of advanced disease and electrical myocardial instability. *PLoS One* 2014;9:e111366. <https://doi.org/10.1371/journal.pone.0111366>; PMID: 25356653.
62. Avanesov M, Münch J, Weinrich J, et al. Prediction of the estimated 5-year risk of sudden cardiac death and syncope or non-sustained ventricular tachycardia in patients with hypertrophic cardiomyopathy using late gadolinium enhancement and extracellular volume CMR. *Eur Radiol* 2017;27:5136–45. <https://doi.org/10.1007/s00330-017-4869-x>; PMID: 28616729.
63. Li Y, Liu X, Yang F, et al. Prognostic value of myocardial extracellular volume fraction evaluation based on cardiac magnetic resonance T1 mapping with T1 long and short in hypertrophic cardiomyopathy. *Eur Radiol* 2021;31:4557–67. <https://doi.org/10.1007/s00330-020-07650-7>; PMID: 33449190.
64. Treibel TA, Fridman Y, Bering P, et al. Extracellular volume associates with outcomes more strongly than native or post-contrast myocardial T1. *JACC Cardiovasc Imaging* 2020;13:44–54. <https://doi.org/10.1016/j.jcmg.2019.03.017>; PMID: 31103587.
65. Dorbala S, Cuddy S, Falk RH. How to image cardiac amyloidosis: a practical approach. *JACC Cardiovasc Imaging* 2020;13:1368–83. <https://doi.org/10.1016/j.jcmg.2019.07.015>; PMID: 31607664.
66. Baggiano A, Boldrini M, Martínez-Naharro A, et al. Noncontrast magnetic resonance for the diagnosis of cardiac amyloidosis. *JACC Cardiovasc Imaging* 2020;13:69–80. <https://doi.org/10.1016/j.jcmg.2019.03.026>; PMID: 31202744.
67. Pan JA, Kerwin MJ, Salerno M. Native T1 mapping, extracellular volume mapping, and late gadolinium enhancement in cardiac amyloidosis: a meta-analysis. *JACC Cardiovasc Imaging* 2020;13:1299–310. <https://doi.org/10.1016/j.jcmg.2020.03.010>; PMID: 32498919.
68. Banyershad SM, Fontana M, Maestrini V, et al. T1 mapping and survival in systemic light-chain amyloidosis. *Eur Heart J* 2015;36:244–51. <https://doi.org/10.1093/eurheartj/ehu444>; PMID: 25411195.
69. Martínez-Naharro A, Treibel TA, Abdel-Gadir A, et al. Magnetic resonance in transthyretin cardiac amyloidosis. *J Am Coll Cardiol* 2017;70:466–77. <https://doi.org/10.1016/j.jacc.2017.05.053>; PMID: 28728692.
70. Martínez-Naharro A, Abdel-Gadir A, Treibel TA, et al. CMR-verified regression of cardiac AL amyloid after chemotherapy. *JACC Cardiovasc Imaging* 2018;11:152–4. <https://doi.org/10.1016/j.jcmg.2017.02.012>; PMID: 28412427.
71. Fontana M, Martínez-Naharro A, Chacko L, et al. Reduction in CMR derived extracellular volume with patisiran indicates cardiac amyloid regression. *JACC Cardiovasc Imaging* 2021;14:189–99. <https://doi.org/10.1016/j.jcmg.2020.07.043>; PMID: 33129740.
72. Sado DM, White SK, Piechnik SK, et al. Identification and assessment of Anderson-Fabry disease by cardiovascular magnetic resonance noncontrast myocardial T1 mapping. *Circ Cardiovasc Imaging* 2013;6:392–8. <https://doi.org/10.1161/CIRCIMAGING.112.000070>; PMID: 23564562.
73. Sado DM, Maestrini V, Piechnik SK, et al. Noncontrast myocardial T1 mapping using cardiovascular magnetic resonance for iron overload. *J Magn Reson Imaging* 2015;41:1505–11. <https://doi.org/10.1002/jmri.24727>; PMID: 25104503.
74. Meloni A, Martini N, Positano V, et al. Myocardial iron overload by cardiovascular magnetic resonance native segmental T1 mapping: a sensitive approach that correlates with cardiac complications. *J Cardiovasc Magn Reson* 2021;23:70. <https://doi.org/10.1186/s12968-021-00765-w>; PMID: 34120634.
75. Corrado D, Basso C, Judge DP. Arrhythmogenic cardiomyopathy. *Circ Res* 2017;121:784–802. <https://doi.org/10.1161/CIRCRESAHA.117.309345>; PMID: 28912183.
76. Corrado D, Perazzolo Marra M, Zorzi A, et al. Diagnosis of arrhythmogenic cardiomyopathy: the Padua criteria. *Int J Cardiol* 2020;319:106–14. <https://doi.org/10.1016/j.ijcard.2020.06.005>; PMID: 32561223.
77. Augusto JB, Eiros R, Nakou E, et al. Dilated cardiomyopathy and arrhythmogenic left ventricular cardiomyopathy: a comprehensive genotype-imaging phenotype study. *Eur Heart J Cardiovasc Imaging* 2020;21:326–36. <https://doi.org/10.1093/ehjci/ezz188>; PMID: 31317183.
78. Aquaro GD, De Luca A, Cappelletto C, et al. Prognostic value of magnetic resonance phenotype in patients with arrhythmogenic right ventricular cardiomyopathy. *J Am Coll Cardiol* 2020;75:2753–65. <https://doi.org/10.1016/j.jacc.2020.04.023>; PMID: 32498802.
79. Aquaro GD, Barison A, Todiére G, et al. Usefulness of combined functional assessment by cardiac magnetic resonance and tissue characterization versus task force criteria for diagnosis of arrhythmogenic right ventricular cardiomyopathy. *Am J Cardiol* 2016;118:1730–6. <https://doi.org/10.1016/j.amjcard.2016.08.056>; PMID: 27825581.
80. Tandri H, Castillo E, Ferrari VA, et al. Magnetic resonance imaging of arrhythmogenic right ventricular dysplasia: sensitivity, specificity, and observer variability of fat detection versus functional analysis of the right ventricle. *J Am Coll Cardiol* 2006;48:2277–84. <https://doi.org/10.1016/j.jacc.2006.07.051>; PMID: 17161260.
81. Bariani R, Cipriani A, Rizzo S, et al. 'Hot phase' clinical presentation in arrhythmogenic cardiomyopathy. *Europace* 2021;23:907–17. <https://doi.org/10.1093/europace/evaa343>; PMID: 33313835.
82. Smith ED, Lakdawala NK, Papoutsidakis N, et al. Desmoplakin cardiomyopathy, a fibrotic and inflammatory form of cardiomyopathy distinct from typical dilated or arrhythmogenic right ventricular cardiomyopathy. *Circulation* 2020;141:1872–84. <https://doi.org/10.1161/CIRCULATIONAHA.119.044934>; PMID: 32372669.
83. Germano G, Kiat H, Kavanagh PB, et al. Automatic quantification of ejection fraction from gated myocardial perfusion SPECT. *J Nucl Med* 1995;36:2138–47. PMID: 7472611.
84. Gimelli A, Liga R, Pasanisi EM, et al. Evaluation of left ventricular diastolic function with a dedicated cadmium-zinc-telluride cardiac camera: comparison with Doppler echocardiography. *Eur Heart J Cardiovasc Imaging* 2014;15:972–9. <https://doi.org/10.1093/ehjci/jeu037>; PMID: 24618658.
85. Koyanagawa K, Naya M, Alkawa T, et al. Prognostic value of phase analysis on gated single photon emission computed tomography in patients with cardiac sarcoidosis. *J Nucl Cardiol* 2021;28:128–36. <https://doi.org/10.1007/s12350-019-01660-9>; PMID: 30815835.
86. Koyanagawa K, Naya M, Alkawa T, et al. The rate of myocardial perfusion recovery after steroid therapy and its implication for cardiac events in cardiac sarcoidosis and primarily preserved left ventricular ejection fraction. *J Nucl Cardiol* 2021;28:1745–56. <https://doi.org/10.1007/s12350-019-01916-4>; PMID: 31605274.
87. Imbricco M, Pellegrino T, Piscopo V, et al. Cardiac sympathetic neuronal damage precedes myocardial fibrosis in patients with Anderson-Fabry disease. *Eur J Nucl Med Mol Imaging* 2017;44:2266–73. <https://doi.org/10.1007/s00259-017-3778-1>; PMID: 28733764.
88. Gimelli A, Aimo A, Vergaro G, et al. Cardiac sympathetic denervation in wild-type transthyretin amyloidosis. *Amyloid* 2020;27:237–43. <https://doi.org/10.1080/13506129.2020.1769059>; PMID: 32441155.
89. Noordzij W, Glaudemans AWJM, van Rheenen RWJ, et al. ¹²³I-labelled metaiodobenzylguanidine for the evaluation of cardiac sympathetic denervation in early stage amyloidosis.

- Eur J Nucl Med Mol Imaging* 2012;39:1609–17. <https://doi.org/10.1007/s00259-012-2187-8>; PMID: 22806059.
90. Hoitsma E, Faber CG, Van Kroonenburgh MJ, et al. Association of small fiber neuropathy with cardiac sympathetic dysfunction in sarcoidosis. *Sarcoidosis Vasc Diffuse Lung Dis* 2005;22:43–50. PMID: 15881279.
 91. Imai E, Kaminaga T, Takada K, et al. Radioactive defect on I-123 MIBG myocardial SPECT imaging in a patient with cardiac sarcoidosis. *Clin Nucl Med* 2002;27:729–30. <https://doi.org/10.1097/00003072-200210000-00011>; PMID: 12352118.
 92. Soussan M, Brillet PY, Nunes H, et al. Clinical value of a high-fat and low-carbohydrate diet before FDG-PET/CT for evaluation of patients with suspected cardiac sarcoidosis. *J Nucl Cardiol* 2013;20:120–7. <https://doi.org/10.1007/s12350-012-9653-3>; PMID: 23188627.
 93. Osborne MT, Hulten EA, Murthy VL, et al. Patient preparation for cardiac fluorine-18 fluorodeoxyglucose positron emission tomography imaging of inflammation. *J Nucl Cardiol* 2017;24:86–99. <https://doi.org/10.1007/s12350-016-0502-7>; PMID: 27277502.
 94. Kobayashi Y, Kumita S, Fukushima Y, et al. Significant suppression of myocardial ¹⁸F-fluorodeoxyglucose uptake using 24-h carbohydrate restriction and a low-carbohydrate, high-fat diet. *J Cardiol* 2013;62:314–9. <https://doi.org/10.1016/j.jjcc.2013.05.004>; PMID: 23810066.
 95. Wollenweber T, Roentgen P, Schäfer A, et al. Characterizing the inflammatory tissue response to acute myocardial infarction by clinical multimodality noninvasive imaging. *Circ Cardiovasc Imaging* 2014;7:811–8. <https://doi.org/10.1161/CIRCIMAGING.114.001689>; PMID: 25049056.
 96. Moriwaki K, Dohi K, Omori T, et al. A survival case of fulminant right-side dominant eosinophilic myocarditis. *Int Heart J* 2017;58:459–62. <https://doi.org/10.1536/ihj.16-338>; PMID: 28496024.
 97. Nensa F, Kloth J, Tezghah E, et al. Feasibility of FDG-PET in myocarditis: comparison to CMR using integrated PET/MRI. *J Nucl Cardiol* 2018;25:785–94. <https://doi.org/10.1007/s12350-016-0616-y>; PMID: 27638745.
 98. Ning N, Guo HH, Iagaru A, et al. Serial cardiac FDG-PET for the diagnosis and therapeutic guidance of patients with cardiac sarcoidosis. *J Card Fail* 2019;25:307–11. <https://doi.org/10.1016/j.cardfail.2019.02.018>; PMID: 30825644.
 99. Saric P, Young KA, Rodriguez-Porcel M, Chareonthaitawee P. PET imaging in cardiac sarcoidosis: a narrative review with focus on novel PET tracers. *Pharmaceuticals (Basel)* 2021;14:1286. <https://doi.org/10.3390/ph14121286>; PMID: 34959686.
 100. Dorbala S, Ando Y, Bokhari S, et al. ASNC/AHA/ASE/EANM/HFSA/ISA/SCMR/SNMMI expert consensus recommendations for multimodality imaging in cardiac amyloidosis: part 1 of 2 – evidence base and standardized methods of imaging. *J Nucl Cardiol* 2019;26:2065–123. <https://doi.org/10.1007/s12350-019-01760-6>; PMID: 31468376.
 101. Trivieri MG, Dweck MR, Abgral R, et al. ¹⁸F-sodium fluoride PET/MR for the assessment of cardiac amyloidosis. *J Am Coll Cardiol* 2016;68:2712–4. <https://doi.org/10.1016/j.jacc.2016.09.953>; PMID: 27978955.
 102. Morgenstern R, Yeh R, Castano A, et al. ¹⁸Fluorine sodium fluoride positron emission tomography, a potential biomarker of transthyretin cardiac amyloidosis. *J Nucl Cardiol* 2018;25:1559–67. <https://doi.org/10.1007/s12350-017-0799-x>; PMID: 28176254.
 103. Ng QKT, Sethi P, Saunders TA, et al. Discordant findings on ¹⁸F-NaF and ^{99m}Tc-HDP bone scans in a patient with ATTR cardiac amyloidosis. *Clin Nucl Med* 2018;43:e89–92. <https://doi.org/10.1097/RLU.0000000000001933>; PMID: 29261619.
 104. Zhang LX, Martineau P, Finnerty V, et al. Comparison of ¹⁸F-sodium fluoride positron emission tomography imaging and ^{99m}Tc-pyrophosphate in cardiac amyloidosis. *J Nucl Cardiol* 2022;29:1132–40. <https://doi.org/10.1007/s12350-020-02425-5>; PMID: 33146862.
 105. Dorbala S, Vangala D, Semer J, et al. Imaging cardiac amyloidosis: a pilot study using ¹⁸F-florbetapir positron emission tomography. *Eur J Nucl Med Mol Imaging* 2014;41:1652–62. <https://doi.org/10.1007/s00259-014-2787-6>; PMID: 24841414.
 106. Vandenberghe R, Van Laere K, Ivanouiu A, et al. ¹⁸F-flutemetamol amyloid imaging in Alzheimer disease and mild cognitive impairment: a phase 2 trial. *Ann Neurol* 2010;68:319–29. <https://doi.org/10.1002/ana.22068>; PMID: 20687209.
 107. Lhommel R, Sempoux C, Ivanouiu A, et al. Is ¹⁸F-flutemetamol PET/CT able to reveal cardiac amyloidosis? *Clin Nucl Med* 2014;39:747–9. <https://doi.org/10.1097/RLU.0000000000000492>; PMID: 24978329.
 108. Dietemann S, Nkoulou R. Amyloid PET imaging in cardiac amyloidosis: a pilot study using ¹⁸F-flutemetamol positron emission tomography. *Ann Nucl Med* 2019;33:624–8. <https://doi.org/10.1007/s12149-019-01372-7>; PMID: 31140154.
 109. Möckelind S, Axelsson J, Pilebro B, et al. Quantification of cardiac amyloid with [¹⁸F]flutemetamol in patients with V30M hereditary transthyretin amyloidosis. *Amyloid* 2020;27:191–9. <https://doi.org/10.1080/135066129.2020.1760237>; PMID: 32400202.
 110. Law WP, Wang WY, Moore PT, et al. Cardiac amyloid imaging with ¹⁸F-florbetaben PET: a pilot study. *J Nucl Med* 2016;57:1733–9. <https://doi.org/10.2967/jnumed.115.169870>; PMID: 27307344.
 111. Genovesi D, Vergaro G, Giorgetti A, et al. Florbetaben PET/CT for differential diagnosis among cardiac immunoglobulin light chain, transthyretin amyloidosis, and mimicking conditions. *JACC Cardiovasc Imaging* 2021;14:246–55. <https://doi.org/10.1016/j.jcmg.2020.05.031>; PMID: 32771577.
 112. Kircher M, Ihne S, Brumberg J, et al. Detection of cardiac amyloidosis with ¹⁸F-florbetaben-PET/CT in comparison to echocardiography, cardiac MRI and DPD-scintigraphy. *Eur J Nucl Med Mol Imaging* 2019;46:1407–16. <https://doi.org/10.1007/s00259-019-04290-y>; PMID: 30798427.
 113. Cademartiri F, Clemente A, Nistri S, Maffei E. Cardiac computed tomography as a complete functional tool. *Eur Heart J Cardiovasc Imaging* 2022;23:485–6. <https://doi.org/10.1093/ehjci/jeab288>; PMID: 34986224.
 114. Seiton S, Clemente A, De Lorenzi C, et al. Cardiac CT perfusion and FFRCTA: pathophysiological features in ischemic heart disease. *Cardiovasc Diagn Ther* 2020;10:1954–78. <https://doi.org/10.21037/cdt-20-414>; PMID: 33381437.
 115. Aziz W, Claridge S, Ntalas I, et al. Emerging role of cardiac computed tomography in heart failure. *ESC Heart Fail* 2019;6:909–20. <https://doi.org/10.1002/ehf2.12479>; PMID: 31400060.
 116. Lee HJ, Im DJ, Youn JC, et al. Assessment of myocardial delayed enhancement with cardiac computed tomography in cardiomyopathies: a prospective comparison with delayed enhancement cardiac magnetic resonance imaging. *Int J Cardiovasc Imaging* 2017;33:577–84. <https://doi.org/10.1007/s10554-016-1024-8>; PMID: 27873128.
 117. Dewey M, Siebes M, Kachelrieß M, et al. Clinical quantitative cardiac imaging for the assessment of myocardial ischaemia. *Nat Rev Cardiol* 2020;17:427–50. <https://doi.org/10.1038/s41569-020-0341-8>; PMID: 32094693.
 118. Scully PR, Bastarrika G, Moon JC, Treibel TA. Myocardial extracellular volume quantification by cardiovascular magnetic resonance and computed tomography. *Curr Cardiol Rep* 2018;20:15. <https://doi.org/10.1007/s11886-018-0961-3>; PMID: 29511861.
 119. Ederly S, Mansencal N, Réant P, et al. Role of multimodality imaging in the diagnosis and management of cardiomyopathies. *Arch Cardiovasc Dis* 2019;112:615–29. <https://doi.org/10.1016/j.acvd.2019.07.004>; PMID: 31607558.
 120. Mitropoulou P, Georgiopoulos G, Figliozzi S, et al. Multimodality imaging in dilated cardiomyopathy: with a focus on the role of cardiac magnetic resonance. *Front Cardiovasc Med* 2020;7:97. <https://doi.org/10.3389/fcvm.2020.00097>; PMID: 32714942.
 121. Schulz-Menger J, Maisch B, Abdel-Aty H, Pankuweit S. Integrated biomarkers in cardiomyopathies: cardiovascular magnetic resonance imaging combined with molecular and immunologic markers – a stepwise approach for diagnosis and treatment. *Herz* 2007;32:458–72. <https://doi.org/10.1007/s00059-007-3046-4>; PMID: 17882371.
 122. Rapezzi C, Quarta CC, Guidalotti PL, et al. Usefulness and limitations of ^{99m}Tc-3,3-diphosphono-1,2-propanodicarboxylic acid scintigraphy in the aetiological diagnosis of amyloidotic cardiomyopathy. *Eur J Nucl Med Mol Imaging* 2011;38:470–8. <https://doi.org/10.1007/s00259-010-1642-7>; PMID: 21069320.
 123. Salinaro F, Meier-Ewert HK, Miller EJ, et al. Longitudinal systolic strain, cardiac function improvement, and survival following treatment of light-chain (AL) cardiac amyloidosis. *Eur Heart J Cardiovasc Imaging* 2017;18:1057–64. <https://doi.org/10.1093/ehjci/jev298>; PMID: 27965280.
 124. Galderisi M, Cardim N, D'Andrea A, et al. The multi-modality cardiac imaging approach to the athlete's heart: an expert consensus of the European Association of Cardiovascular Imaging. *Eur Heart J Cardiovasc Imaging* 2015;16:353. <https://doi.org/10.1093/ehjci/jev323>; PMID: 25681828.
 125. Malik N, Mukherjee M, Wu KC, et al. Multimodality imaging in arrhythmogenic right ventricular cardiomyopathy. *Circ Cardiovasc Imaging* 2022;15:e013725. <https://doi.org/10.1161/CIRCIMAGING.121.013725>; PMID: 35147040.
 126. Authors/Task Force members, Elliott PM, Anastasakis A, et al. 2014 ESC Guidelines on diagnosis and management of hypertrophic cardiomyopathy: the Task Force for the Diagnosis and Management of Hypertrophic Cardiomyopathy of the European Society of Cardiology (ESC). *Eur Heart J* 2014;35:2733–79. <https://doi.org/10.1093/eurheartj/ehu284>; PMID: 25173338.
 127. Towbin JA, McKenna WJ, Abrams DJ, et al. 2019 HRS expert consensus statement on evaluation, risk stratification, and management of arrhythmogenic cardiomyopathy: executive summary. *Heart Rhythm* 2019;16:e373–407. <https://doi.org/10.1016/j.hrthm.2019.09.019>; PMID: 31676023.
 128. Porcari A, Baggio C, Fabris E, et al. Endomyocardial biopsy in the clinical context: current indications and challenging scenarios. *Heart Fail Rev* 2023;28:123–35. <https://doi.org/10.1007/s10741-022-10247-5>; PMID: 35567705.
 129. Wang W, Murray B, Tichnell C, et al. Clinical characteristics and risk stratification of desmoplakin cardiomyopathy. *Europace* 2022;24:268–77. <https://doi.org/10.1093/europace/ekab183>; PMID: 34352074.
 130. Protonotarios A, Wicks E, Ashworth M, et al. Prevalence of ¹⁸F-fluorodeoxyglucose positron emission tomography abnormalities in patients with arrhythmogenic right ventricular cardiomyopathy. *Int J Cardiol* 2019;284:99–104. <https://doi.org/10.1016/j.ijcard.2018.10.083>; PMID: 30409737.